

Revisiting a Fast Newton Solver for a 2-D Spectral Estimation Problem: Computations with the Full Hessian

Ji Cheng and Bin Zhu *

* School of Intelligent Systems Engineering, Sun Yat-sen University,
Gongchang Road 66, 518107 Shenzhen, China (e-mails:
chengj227@mail2.sysu.edu.cn, zhub26@mail.sysu.edu.cn)

Abstract:

Spectral estimation plays a fundamental role in frequency-domain identification and related signal processing problems. This paper revisits a 2-D spectral estimation problem formulated in terms of convex optimization. More precisely, we work with the dual optimization problem and show that the full Hessian of the dual function admits a Toeplitz-block Toeplitz structure which is consistent with our finding in a previous work. This particular structure of the Hessian enables a fast inversion algorithm in the solution of the dual optimization problem via Newton's method whose superior speed of convergence is illustrated via simulations.

Keywords: Two-dimensional spectral estimation, moment problem, convex optimization, Newton's method, Toeplitz-block Toeplitz matrix, fast algorithm.

1. INTRODUCTION

Spectral estimation is about inferring the statistical power distribution of a random process/field in the frequency domain from a finite number of samples. It has vast applications in e.g., system identification (Ringh et al., 2015, 2018; Zhu and Zorzi, 2024b), radar signal processing (Engels et al., 2017; Zhu et al., 2019, 2021b), texture image generation (Lindquist and Picci, 2016), and geotechnical modeling (Zhu et al., 2023).

Among different methods for spectral estimation, there is a series of works that center around the idea of *rational covariance extension*, see e.g., Byrnes et al. (1998, 2000, 2001); Georgiou and Lindquist (2003); Ferrante et al. (2008, 2012); Zorzi (2014b,a); Zhu et al. (2021a); Zhu and Zorzi (2023, 2024a). In those works, spectral estimation is formulated as equality constrained optimization problems in which the constraints are *trigonometric moment equations* for the spectral density, and the objective functional is usually some kind of entropy or a related concept of divergence. These optimization problems are successful because they can be made well-posed and allow for solution tuning by smoothly changing the parameters.

In a recent work Zhu and Liu (2022), a spectral estimation problem for two-dimensional (2-D) random fields was considered using the *Itakura-Saito* (IS) pseudo-distance (Ferrante et al., 2012) as the objective functional in the optimization. The problem was solved via duality, and

the Hessian of the dual function was shown to have a *Toeplitz-block Toeplitz* (TBT) structure (Wax and Kailath, 1983) which makes possible a fast Newton algorithm. However, only a principal submatrix of the full Hessian was computed in that paper, and thus strictly speaking, the algorithm should be interpreted as a *quasi-Newton* method (Kreutz-Delgado, 2009) which in general, converges slower than the true Newton's method. This last observation motivates the investigation in this paper. Indeed, we show that the TBT structure of the full Hessian is preserved if we collect the dual variables in a suitable order. Hence the fast inversion algorithm in Wax and Kailath (1983) can be used provided that proper modifications are made for Hermitian matrices. In addition, we give numerical examples in which Newton's method, enabled by the fast inversion algorithm for the full Hessian, converges much faster than the quasi-Newton method in Zhu and Liu (2022).

The remaining part of this paper is organized as follows. Sec. 2 gives a brief review of a 2-D spectral estimation problem formulated in terms of optimization. Sec. 3 characterizes the algebraic structure of the full Hessian of the dual objective function. Sec. 4 describes a fast inversion algorithm for the structured Hessian, and Sec. 5 treats the computation of the Newton direction, i.e., solving linear equations where the Hessian is the coefficient matrix. Sec. 6 provides simulation results. Sec. 7 concludes the paper.

* This work was supported in part by the National Natural Science Foundation of China (No. 62103453) and the Innovation Training Program for College Students of Sun Yat-sen University (No. 20252496).

2. REVIEW OF A 2-D SPECTRAL ESTIMATION PROBLEM

We focus on the spectral estimation problem for complex-valued zero-mean wide-sense stationary 2-D random field $\{y_t : t = (t_1, t_2) \in \mathbb{Z}^2\}$. The assumption of stationarity implies that the (auto-)covariance of the random field $\sigma_{\mathbf{k}} := \mathbb{E} y_{t+\mathbf{k}} \bar{y}_t$ is a function of the difference $\mathbf{k} \in \mathbb{Z}^2$ between the vectorial indices only. Here \mathbb{E} denotes the mathematical expectation and \bar{z} signifies the complex conjugate of $z \in \mathbb{C}$. The (power) spectral density of the random field is obtained by taking the Fourier transform of the covariance function $\sigma_{\mathbf{k}}$, i.e.,

$$\Phi(\boldsymbol{\theta}) := \sum_{\mathbf{k} \in \mathbb{Z}^2} \sigma_{\mathbf{k}} e^{-i\langle \mathbf{k}, \boldsymbol{\theta} \rangle}, \quad (1)$$

where $\boldsymbol{\theta} = (\theta_1, \theta_2)$ such that each θ_j , $j = 1, 2$ is an angular frequency in the interval $\mathbb{T} := [0, 2\pi]$, and $\langle \mathbf{k}, \boldsymbol{\theta} \rangle := k_1 \theta_1 + k_2 \theta_2$ is the inner product in \mathbb{R}^2 . Conversely, the covariance $\sigma_{\mathbf{k}}$ is the \mathbf{k} -th Fourier coefficient of $\Phi(\boldsymbol{\theta})$, namely

$$\sigma_{\mathbf{k}} = \int_{\mathbb{T}^2} e^{i\langle \mathbf{k}, \boldsymbol{\theta} \rangle} \Phi(\boldsymbol{\theta}) dm(\boldsymbol{\theta}), \quad (2)$$

where $dm(\boldsymbol{\theta}) = \frac{1}{(2\pi)^2} d\theta_1 d\theta_2$ is the normalized Lebesgue measure in \mathbb{T}^2 . Therefore, Φ represents a frequency-domain description of the random field which encodes all the second-order statistics. When the random field is Gaussian, the spectral density in fact specifies the probability distribution of any finite collection of random variables from the field.

The *trigonometric moment equation* (2) above plays a fundamental role in a class of spectral estimation methods called *rational covariance extension*. Within that philosophy, one aims to reconstruct a rational spectral density Φ as a solution to (2) given a finite number of covariances $\{\sigma_{\mathbf{k}}\}_{\mathbf{k} \in \Lambda}$ where $\Lambda \subset \mathbb{Z}^2$ is an index set. A typical choice of the index set is simply a “rectangle” which will be used throughout this paper:

$$\Lambda = \{\mathbf{k} = (k_1, k_2) \in \mathbb{Z}^2 : |k_j| \leq n_j, j = 1, 2\}, \quad (3)$$

where n_1 and n_2 are positive integers. In practice we often observe a finite realization (samples) of the random field

$$\{y_t : t_j \in [0, T_j - 1] \cap \mathbb{Z}, j = 1, 2\} \quad (4)$$

where positive integers T_1 and T_2 specify the sample size, and the covariances $\{\sigma_{\mathbf{k}}\}_{\mathbf{k} \in \Lambda}$ are estimated from the realization with standard formulas, see Stoica and Moses (2005, p. 23) and Zhu et al. (2021b). These estimates are reliable when each positive integer n_j is significantly smaller than T_j .

Our specific problem setup is taken from Zhu and Liu (2022) which is a specialization of the work in Zhu et al. (2021b,a) by fixing the dimension $d = 2$. More precisely, we set up the following *primal* optimization problem

$$\begin{aligned} \min_{\Phi > 0} D(\Phi, \Psi) &:= \int_{\mathbb{T}^2} [\log(\Phi^{-1}\Psi) + \Psi^{-1}(\Phi - \Psi)] dm \\ \text{s.t. } \sigma_{\mathbf{k}} &= \int_{\mathbb{T}^2} e^{i\langle \mathbf{k}, \boldsymbol{\theta} \rangle} \Phi dm \quad \forall \mathbf{k} \in \Lambda, \end{aligned} \quad (5)$$

where the Itakura-Saito (IS) pseudo-distance (Ferrante et al., 2012; Lindquist and Picci, 2015) is utilized as the objective functional and moment equations are included as equality constraints. The additional element in the problem, Ψ , called *prior*, contains some *a priori* information

about the desired solution so that one tries to find a Φ as close as possible to Ψ according to the IS pseudo-distance that meets the moment constraints. Notice that in (5) and the remaining part of this paper, the integral variable $\boldsymbol{\theta}$ is omitted when there is no risk of confusion.

The primal problem (5) is solved via duality. More precisely, the dual optimization problem is written as

$$\min_{\mathbf{Q} \in \mathcal{L}_+} J_{\Psi}(\mathbf{Q}) := \langle \mathbf{Q}, \boldsymbol{\Sigma} \rangle - \int_{\mathbb{T}^2} \log(\Psi^{-1} + Q) dm \quad (6)$$

where, the dual variable $\mathbf{Q} = \{q_{\mathbf{k}}\}_{\mathbf{k} \in \Lambda}$ consists of the Lagrange multipliers such that $q_{-\mathbf{k}} = \bar{q}_{\mathbf{k}}$ for all $\mathbf{k} \in \Lambda$ and $q_0 \in \mathbb{R}$, $\boldsymbol{\Sigma} = \{\sigma_{\mathbf{k}}\}_{\mathbf{k} \in \Lambda}$ contains all the covariances in the equality constraints of (5), $\langle \mathbf{Q}, \boldsymbol{\Sigma} \rangle := \sum_{\mathbf{k} \in \Lambda} q_{\mathbf{k}} \bar{\sigma}_{\mathbf{k}}$ defines a real-valued inner product between two symmetric multisequences indexed in Λ , $Q(\boldsymbol{\theta}) := \sum_{\mathbf{k} \in \Lambda} q_{\mathbf{k}} e^{-i\langle \mathbf{k}, \boldsymbol{\theta} \rangle}$ is a symmetric trigonometric polynomial with coefficients in \mathbf{Q} , and the feasible set is given by

$$\mathcal{L}_+ := \{\mathbf{Q} : (\Psi^{-1} + Q)(\boldsymbol{\theta}) > 0 \quad \forall \boldsymbol{\theta} \in \mathbb{T}^2\}. \quad (7)$$

We remark that \mathbf{Q} dwells in a vector space of *real* dimension $|\Lambda| = (2n_1 + 1)(2n_2 + 1)$ where $|\cdot|$ denotes the cardinality of a set. The dual problem (6) is strictly convex Zhu et al. (2021b). Given the optimal solution $\hat{\mathbf{Q}}$ to the dual problem, the optimal solution to the primal problem can be recovered as $\hat{\Phi} = (\Psi^{-1} + \hat{\mathbf{Q}})^{-1}$.

3. ALGEBRAIC STRUCTURE OF THE FULL HESSIAN

In this section, we investigate the proper algebraic structure of the full Hessian that will enable the true Newton’s method to solve the dual problem (6). Since the specific index set Λ in (3) is used in our optimization problem, we can identify the dual variable as a $(2n_2 + 1) \times (2n_1 + 1)$ complex matrix

$$\mathbf{Q} = \begin{bmatrix} q_{-n_1, -n_2} & \cdots & q_{0, -n_2} & \cdots & q_{n_1, -n_2} \\ \vdots & & \vdots & & \vdots \\ q_{-n_1, 0} & \cdots & q_{0, 0} & \cdots & q_{n_1, 0} \\ \vdots & & \vdots & & \vdots \\ q_{-n_1, n_2} & \cdots & q_{0, n_2} & \cdots & q_{n_1, n_2} \end{bmatrix}. \quad (8)$$

In order to properly express the gradient and Hessian of the dual function J_{Ψ} , let us introduce the usual *vectorization* of the matrix \mathbf{Q} above by stacking the columns one by one, that is, column 1 on the top, column 2 below column 1, column 3 below column 2, etc., and denote the operation as

$$\mathbf{q} := \text{vec}(\mathbf{Q}). \quad (9)$$

The vector \mathbf{q} has a size of $|\Lambda|$, and q_{k_1, k_2} occupies the $[(2n_2 + 1)(k_1 + n_1) + k_2 + n_2 + 1]$ -th entry. In fact, this corresponds to the *lexicographic* order of the index set Λ . Moreover, we write $[\mathbf{q}]_j$ for the j -th entry of \mathbf{q} . With an abuse of notation, we shall rewrite the dual function in (6) as $J_{\Psi}(\mathbf{q})$ and define the *gradient* as the $|\Lambda|$ -dimensional vector

$$\nabla J_{\Psi}(\mathbf{q}) := \frac{\partial J_{\Psi}(\mathbf{q})}{\partial \mathbf{q}} \text{ such that } [\nabla J_{\Psi}(\mathbf{q})]_j = \frac{\partial J_{\Psi}(\mathbf{q})}{\partial [\mathbf{q}]_j}. \quad (10)$$

For each $j = 1, \dots, |\Lambda|$, the last term in the above formula admits the expression

$$\frac{\partial J_{\Psi}(\mathbf{q})}{\partial q_{\mathbf{k}}} = \sigma_{-\mathbf{k}} - \int_{\mathbb{T}^2} e^{-i\langle \mathbf{k}, \boldsymbol{\theta} \rangle} (\Psi^{-1} + Q)^{-1} dm \quad (11)$$

for a unique $\mathbf{k} \in \Lambda$, see Zhu et al. (2021b). This is known as the *Wirtinger derivative* (Hörmander, 1990) of J_Ψ in which the conjugate pair $q_{\mathbf{k}}$ and $\bar{q}_{\mathbf{k}}$ are viewed as formally independent variables in calculations.

The second-order partial derivatives can be computed in a similar fashion, and the formula is given by

$$\begin{aligned} \frac{\partial^2 J_\Psi(\mathbf{q})}{\partial \bar{q}_{\ell} \partial q_{\mathbf{k}}} &:= \frac{\partial}{\partial \bar{q}_{\ell}} \left[\frac{\partial J_\Psi(\mathbf{q})}{\partial q_{\mathbf{k}}} \right] \\ &= \int_{\mathbb{T}^2} e^{i\langle \ell - \mathbf{k}, \theta \rangle} (\Psi^{-1} + Q)^{-2} dm. \end{aligned} \quad (12)$$

It is then natural to organize the second-order partials into a $|\Lambda| \times |\Lambda|$ *Hessian* matrix

$$\mathcal{H}(\mathbf{q}) := \frac{\partial}{\partial \bar{\mathbf{q}}} \left[\frac{\partial J_\Psi(\mathbf{q})}{\partial \mathbf{q}} \right] \text{ with } [\mathcal{H}(\mathbf{q})]_{jk} = \frac{\partial}{\partial [\bar{\mathbf{q}}]_k} \left[\frac{\partial J_\Psi(\mathbf{q})}{\partial [\mathbf{q}]_j} \right] \quad (13)$$

where each entry $[\mathcal{H}(\mathbf{q})]_{jk}$ correspond to (12) for a unique pair $(\mathbf{k}, \ell) \in \Lambda^2$. The Hessian $\mathcal{H}(\mathbf{q})$ is shown to be (Hermitian) positive definite (Zhu et al., 2021b, Sec. 3.1). The partial Hessian described in Zhu and Liu (2022, Eq. (31)) is in fact a lower-right principal submatrix of $\mathcal{H}(\mathbf{q})$ of size $n_2 + 1 + n_1(2n_2 + 1) \approx |\Lambda|/2$.

We observe that the second-order partials depend on the difference $\ell - \mathbf{k}$ of the indices. Hence for a feasible \mathbf{q} and any $\mathbf{k} \in \mathbb{Z}^2$, we can define a complex-valued function

$$h_{\mathbf{k}}(\mathbf{q}) := \int_{\mathbb{T}^2} e^{i\langle \mathbf{k}, \theta \rangle} (\Psi^{-1} + Q)^{-2} dm. \quad (14)$$

Then the Hessian can be viewed as a Hermitian block-Toeplitz matrix

$$\mathcal{H} = \begin{bmatrix} \mathbf{R}_0 & \mathbf{R}_1 & \dots & \mathbf{R}_{2n_1} \\ \mathbf{R}_1^* & \ddots & \ddots & \vdots \\ \vdots & \ddots & \ddots & \mathbf{R}_1 \\ \mathbf{R}_{2n_1}^* & \dots & \mathbf{R}_1^* & \mathbf{R}_0 \end{bmatrix} \quad (15a)$$

with $2n_1 + 1$ blocks in each row (and column) where each block

$$\mathbf{R}_j = \begin{bmatrix} h_{j,0} & h_{j,1} & \dots & h_{j,2n_2} \\ h_{j,-1} & \ddots & \ddots & \vdots \\ \vdots & \ddots & \ddots & h_{j,1} \\ h_{j,-2n_2} & \dots & h_{j,-1} & h_{j,0} \end{bmatrix} \quad (15b)$$

is a square Toeplitz matrix of size $2n_2 + 1$. For simplicity, we have omitted the dependence on \mathbf{q} in (15). Such a structure of \mathcal{H} is called Toeplitz-block Toeplitz in Wax and Kailath (1983), and TBT for short. It follows that in practical calculations, only the first block row of the Hessian needs to be computed.

4. FAST INVERSION OF THE STRUCTURED HESSIAN

To simplify the discussion, let us consider the case $n_1 = n_2 = n$ for some positive integer n , and take $p = 2n + 1$ for the size of each block in (15b). We can now define a sequence of matrices $\{\mathcal{H}_j\}_{j \geq 0}$ of increasing size such that $\mathcal{H}_0 = \mathbf{R}_0$, and

$$\mathcal{H}_j = \begin{bmatrix} \mathbf{R}_0 & \mathbf{R}_1 & \dots & \mathbf{R}_{2j} \\ \mathbf{R}_1^* & \ddots & \ddots & \vdots \\ \vdots & \ddots & \ddots & \mathbf{R}_1 \\ \mathbf{R}_{2j}^* & \dots & \mathbf{R}_1^* & \mathbf{R}_0 \end{bmatrix} \quad \text{for } j \geq 1. \quad (16)$$

Clearly $\{\mathcal{H}_j\}_{j \geq 0}$ has a nested structure in the sense that \mathcal{H}_j is a principal submatrix of \mathcal{H}_{j+1} for all $j \geq 0$. A more precisely statement can be made as follows. Let us define

$$\underline{\mathbf{R}}_k := \begin{bmatrix} \mathbf{R}_k \\ \vdots \\ \mathbf{R}_1 \end{bmatrix}, \quad k = 1, 2, \dots, \quad (17)$$

and an accompanying sequence of matrices of increasing size $\{\mathcal{G}_k\}_{k \geq 0}$ by $\mathcal{G}_0 = \mathbf{R}_0$ and

$$\mathcal{G}_k = \begin{bmatrix} \mathcal{G}_{k-1} & \mathbf{R}_k \\ \underline{\mathbf{R}}_k^* & \mathbf{R}_0 \end{bmatrix}, \quad k = 1, 2, \dots \quad (18)$$

Then we have

$$\mathcal{H}_j = \mathcal{G}_{2j}, \quad j = 1, 2, \dots \quad (19)$$

The nested structure is reflected in (18).

Fast inversion of TBT matrices has been studied in Wax and Kailath (1983), and the main idea is to invert a sequence of nested TBT matrices $\{\mathcal{G}_k\}_{k \geq 0}$, using the computed inverse of \mathcal{G}_{k-1} to facilitate the computation of \mathcal{G}_k^{-1} . The algorithm is briefly reviewed next. Notice that our \mathcal{H}_j and \mathcal{G}_k are Hermitian, which can bring about additional saving. Also, the inversion of our Hessian (15a), which is now \mathcal{H}_n in view of (16), follows an identical procedure because of (19).

A fundamental property of TBT matrices is that they are symmetric with respect to the antidiagonal, i.e., the diagonal connecting the lower-left and upper-right corners of a square matrix. Such a property is called *persymmetry* in Wax and Kailath (1983, Lemma 1), and is described mathematically by the formula

$$\mathcal{G}_k = J_{p,k+1} \mathcal{G}_k^\top J_{p,k+1}, \quad (20)$$

where $J_{p,k}$ is the $pk \times pk$ permutation matrix (Zohar, 1969)

$$J_{p,k} = \begin{bmatrix} & & & J_p \\ & & \ddots & \\ & \ddots & & \\ J_p & & & \end{bmatrix} \quad (21a)$$

with $k \times k$ blocks and each block J_p is the $p \times p$ permutation matrix

$$J_p = \begin{bmatrix} & & & 1 \\ & \ddots & & \\ 1 & & & \end{bmatrix}. \quad (21b)$$

Using block elimination, the block matrix in (18) admits a block inverse

$$\mathcal{G}_k^{-1} = \begin{bmatrix} \mathcal{G}_{k-1}^{-1} + \underline{W}_k \alpha_k^{-1} \underline{W}_k^* & \underline{W}_k \alpha_k^{-1} \\ \alpha_k^{-1} \underline{W}_k^* & \alpha_k^{-1} \end{bmatrix} \quad (22a)$$

where

$$\underline{W}_k := -\mathcal{G}_{k-1}^{-1} \underline{\mathbf{R}}_k \quad (22b)$$

and

$$\alpha_k := \mathbf{R}_0 + \underline{W}_k^* \underline{\mathbf{R}}_k \quad (22c)$$

is the *Schur complement* $\mathcal{G}_k / \mathcal{G}_{k-1}$. Now let us take inverse of both sides of the equation in (20), and we have

$$\begin{aligned}\mathcal{G}_k^{-1} &= J_{p,k+1} \mathcal{G}_k^{-\top} J_{p,k+1} \\ &= \begin{bmatrix} J_p \boldsymbol{\alpha}_k^{-\top} J_p & J_p \boldsymbol{\alpha}_k^{-\top} \widehat{W}_k^\top \\ \widehat{W}_k \boldsymbol{\alpha}_k^{-\top} J_p & \mathcal{G}_{k-1}^{-1} + \widehat{W}_k \boldsymbol{\alpha}_k^{-\top} \widehat{W}_k^\top \end{bmatrix},\end{aligned}\quad (23)$$

where, the second equality follows from direct computation with (21a) and (22a), \widehat{A} denotes elementwise complex conjugate of a matrix A , and

$$\widehat{W}_k := J_{p,k} W_k \quad (24)$$

with W_k in (22b).

From the two representation of \mathcal{G}_k^{-1} (22a) and (23), we can read out two equations between the blocks

$$(\mathcal{G}_k^{-1})_{i,j} = (\mathcal{G}_{k-1}^{-1} + W_k \boldsymbol{\alpha}_k^{-1} W_k^*)_{i,j}, \quad i, j = 1, \dots, k, \quad (25)$$

and

$$(\mathcal{G}_k^{-1})_{i+1,j+1} = \left(\mathcal{G}_{k-1}^{-1} + \widehat{W}_k \boldsymbol{\alpha}_k^{-\top} \widehat{W}_k^\top \right)_{i,j}, \quad i, j = 1, \dots, k, \quad (26)$$

where the subscripts i and j refer to blocks. Combining (25) and (26), the blocks of \mathcal{G}_{k-1}^{-1} can be eliminated, and we are left with a recursion among blocks of \mathcal{G}_k^{-1} :

$$(\mathcal{G}_k^{-1})_{i+1,j+1} = (\mathcal{G}_k^{-1})_{i,j} + (\mathcal{W}_k)_{i,j}, \quad i, j = 1, \dots, k. \quad (27)$$

where $\mathcal{W}_k := \widehat{W}_k \boldsymbol{\alpha}_k^{-\top} \widehat{W}_k^\top - W_k \boldsymbol{\alpha}_k^{-1} W_k^*$ is a $k \times k$ block matrix. If we introduce the new notation

$$\widehat{\mathbf{R}}_j := J_p \mathbf{R}_j, \quad j = 1, 2, \dots, \quad (28a)$$

and

$$\widehat{\mathbf{R}}_k := J_{p,k} \underline{\mathbf{R}}_k = \begin{bmatrix} \widehat{\mathbf{R}}_1 \\ \vdots \\ \widehat{\mathbf{R}}_k \end{bmatrix}, \quad k = 1, 2, \dots, \quad (28b)$$

where $\underline{\mathbf{R}}_k$ was defined in (17), then according to Formulas (13a), (13c), and (17) in Wax and Kailath (1983), the recursions for \widehat{W}_k and $\boldsymbol{\alpha}_k$ are given as follows:

$$\widehat{W}_{k+1} = \begin{bmatrix} \widehat{W}_k \\ \mathbf{0}_p \end{bmatrix} - \begin{bmatrix} \widehat{W}_k \\ I_p \end{bmatrix} \boldsymbol{\alpha}_k^{-\top} \boldsymbol{\beta}_k, \quad (29a)$$

and

$$\boldsymbol{\alpha}_{k+1} = \boldsymbol{\alpha}_k - \boldsymbol{\beta}_k^* \boldsymbol{\alpha}_k^{-\top} \boldsymbol{\beta}_k, \quad (29b)$$

where

$$\boldsymbol{\beta}_k = W_k^\top \widehat{\mathbf{R}}_k + \widehat{\mathbf{R}}_{k+1}. \quad (29c)$$

The pseudocode for the inversion of our structured Hessian is given in Algorithm 1. Notice that due to the Hermitian and persymmetric structure of \mathcal{G}_k^{-1} , roughly only a quarter of the blocks need to be computed, and this point is also illustrated in Algorithm 1.

5. FAST SOLUTION TO TBT SYSTEMS OF LINEAR EQUATIONS

Fast solution to TBT systems of linear equations was also studied in Wax and Kailath (1983). Here we slightly expand their results to the case in which the unknown and the right-hand matrices can have an arbitrary number of columns. To this end, consider the linear equations

$$\mathcal{H}_n \underline{X}_{2n} = \underline{B}_{2n} \quad (30)$$

where \mathcal{H}_n is the TBT Hessian matrix in (15a), and \underline{X}_{2n} (unknown) and \underline{B}_{2n} (known) are $p^2 \times q$ matrices.

Algorithm 1 Inversion of the Hessian $\mathcal{H}_n = \mathcal{G}_{2n}$

Require: A Hessian matrix of the form (15).

```

1:  $\mathcal{G}_0^{-1} \leftarrow \mathbf{R}_0^{-1}$ .
2: Compute  $\underline{W}_1$ ,  $\boldsymbol{\alpha}_1$  by (22).
3: Compute  $\widehat{W}_1$ ,  $\underline{\mathbf{R}}_1$  by (24) and (28b), respectively.
4: while  $1 \leq k \leq 2n - 1$  do
5:   Compute  $\widehat{\mathbf{R}}_{k+1}$  by (28a).
6:   Update  $\boldsymbol{\beta}_k$  by (29c).
7:   Update  $\boldsymbol{\alpha}_{k+1}$  by (29b).
8:   Update  $\widehat{W}_{k+1}$  by (29a).
9: end while
10:  $\mathcal{G}_{2n}^{-1} \leftarrow p^2 \times p^2$  zero matrix.
11: Update the first block row of  $\mathcal{G}_{2n}^{-1}$  by

$$(\mathcal{G}_k^{-1})_{1,1} = J_p \boldsymbol{\alpha}_k^{-\top} J_p \text{ and } (\mathcal{G}_k^{-1})_{1,2:k+1} = J_p \boldsymbol{\alpha}_k^{-\top} \widehat{W}_k^\top.$$

12: Recover  $\underline{W}_{2n} = J_{p,2n} \widehat{W}_{2n}$ .
13: // Update the upper quarter of  $\mathcal{G}_{2n}^{-1}$ .
14: for  $i = 1 : n$  do
15:   for  $j = i : 2n - i$  do
16:     Update  $(\mathcal{G}_{2n}^{-1})_{i+1,j+1}$  by (27).
17:   end for
18: end for
19: // Halve the diagonal and antidiagonal
   elements of  $\mathcal{G}_{2n}^{-1}$ . Notice that the center
   block  $(\mathcal{G}_{2n}^{-1})_{n+1,n+1}$  gets quartered.
20: for  $i = 1 : n + 1$  do
21:    $(\mathcal{G}_{2n}^{-1})_{i,i} \leftarrow \frac{1}{2} (\mathcal{G}_{2n}^{-1})_{i,i}$ .
22:    $(\mathcal{G}_{2n}^{-1})_{i,2n+2-i} \leftarrow \frac{1}{2} (\mathcal{G}_{2n}^{-1})_{i,2n+2-i}$ .
23: end for
24: // Update the right quarter of  $\mathcal{G}_{2n}^{-1}$  by
   persymmetry.
25:  $\mathcal{G}_{2n}^{-1} \leftarrow \mathcal{G}_{2n}^{-1} + (J_{p,2n+1} \mathcal{G}_{2n}^{-1} J_{p,2n+1})^\top$ .
26: // Update the block lower triangular part of
    $\mathcal{G}_{2n}^{-1}$  by Hermitianity.
27:  $\mathcal{G}_{2n}^{-1} \leftarrow \mathcal{G}_{2n}^{-1} + (\mathcal{G}_{2n}^{-1})^*$ .
28: return  $\mathcal{G}_{2n}^{-1}$ .
```

Apparently, \underline{X}_{2n} and \underline{B}_{2n} can be viewed as $p \times 1$ block vectors where each block has a size of $p \times q$.

Note that due to the relation (19) and the nested structure (18), we can define a sequence of equations

$$\mathcal{G}_k \underline{X}_k = \underline{B}_k, \quad 0 \leq k \leq 2n, \quad (31)$$

where \mathcal{G}_k has been defined in (18), \underline{B}_k is formed by the leading $k+1$ blocks of the block vector \underline{B}_{2n} , and \underline{X}_k is an unknown matrix of size $(k+1)p \times q$. Notice that in general \underline{X}_k is not equal to the leading $k+1$ blocks of \underline{X}_{2n} , and only when $k = 2n$ we obtain the solution \underline{X}_{2n} to (30).

Using (22) we can derive the formula

$$\underline{X}_{k+1} = \begin{bmatrix} \underline{X}_k \\ \mathbf{0}_{p \times q} \end{bmatrix} + \begin{bmatrix} W_k \\ I_p \end{bmatrix} \boldsymbol{\alpha}_k^{-1} \boldsymbol{\delta}_k \quad (32a)$$

and

$$\boldsymbol{\delta}_k = W_k^* \underline{B}_k + B_{k+1}, \quad 0 \leq k \leq 2n - 1, \quad (32b)$$

where B_k (without underline) is the $(k+1)$ -th block of the block vector \underline{B}_{2n} , and W_k and $\boldsymbol{\alpha}_k$ are updated via (24), (29a), and (29b). We summarize the pseudocode for the fast solution to TBT systems of linear equations in Algorithm 2.

Algorithm 2 Solving the TBT system (30) of equations

Require: A Hessian matrix of the form (15a) and a $p^2 \times q$ matrix B_{2n} .

- 1: $[\underline{X}_0 \ \underline{W}_1] \leftarrow \mathbf{R}_0 \setminus [B_0 \ -\mathbf{R}_1]$.
- 2: Compute α_1 by (22c).
- 3: Compute \widehat{W}_1 , $\widehat{\mathbf{R}}_1$ by (24) and (28b), respectively.
- 4: **while** $1 \leq k \leq 2n - 1$ **do**
- 5: Update δ_k by (32b).
- 6: Update \underline{X}_k by (32a).
- 7: Compute $\widehat{\mathbf{R}}_{k+1}$ by (28a).
- 8: Update β_k by (29c).
- 9: Update α_{k+1} by (29b).
- 10: Update \widehat{W}_{k+1} by (29a).
- 11: **end while**
- 12: Compute δ_{2n} by (32b).
- 13: Compute \underline{X}_{2n} by (32a).
- 14: **return** \underline{X}_{2n} .

6. SIMULATIONS

In this section, we perform numerical simulations for the fast inversion of positive definite TBT matrices and for the solution of the dual problem (6) using Newton's method with the full Hessian. The results are divided into two subsections.

6.1 Testing Algorithm 1

The first set of numerical experiments are about the inversion of positive definite TBT matrices. In accordance with the previous sections, the size parameters are set as $n_1 = n_2 = n$, resulting in $p^2 \times p^2$ TBT matrices of the form (15) with $p = 2n + 1$. Each TBT matrix is randomly generated and is made positive definite by adding a positive multiple of the identity matrix. Then two methods are compared for the inversion of such a TBT matrix, namely Algorithm 1 for fast inversion and the direct inversion using the MATLAB command \mathbf{A}^{-1} for any square matrix \mathbf{A} . We compute these inverses for values of n ranging from 1 to 40. Each each n , twenty positive definite TBT matrices are generated and the running times of the two methods are averaged and shown in Fig. 1. Notice that we only present the running times for $20 < n \leq 40$, because for $n \leq 20$, both methods yield nearly identical results. We see that Algorithm 1 outperforms the direction inversion when matrix size is large, in particular, when $n \geq 30$. The advantage of the fast algorithm can be explained theoretically. Indeed, according to Wax and Kailath (1983), the computational complexity of Algorithm 1 is $O(p^5)$, see also Akaike (1973), while the direct inversion has a complexity of $O(p^6)$, the usual cubic complexity applied to a square matrix of size p^2 .

6.2 Full Hessian vs. quarter Hessian in Newton's method

In this subsection, we use Newton's method with the full Hessian to solve the dual problem (6), and make a comparison with the quasi-Newton method in Zhu and Liu (2022) which involves only a quarter Hessian, see the discussion after (13).

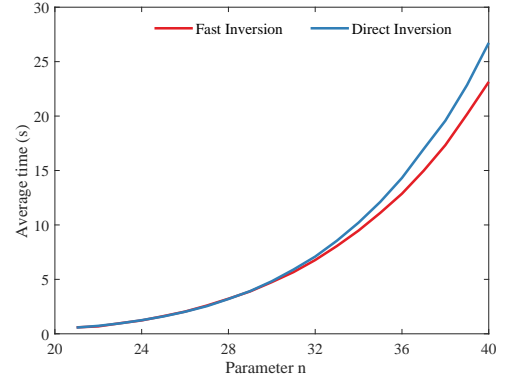


Fig. 1. Algorithm 1 vs. the direction method for the inversion of positive definite TBT matrices: average running times for n ranging from 21 to 40.

In our implementation, all integrals against the normalized Lebesgue measure such as those in (6), (11), and (12) are discretized as Riemann sums:

$$\int_{\mathbb{T}^2} f dm \approx \frac{1}{N_1 N_2} \sum_{\theta \in \mathbb{T}_N^2} f(\theta), \quad (33)$$

where $\mathbb{T}_N^2 := \left\{ \left(\frac{2\pi}{N_1} \ell_1, \frac{2\pi}{N_2} \ell_2 \right) : \ell_j \in [0, N_j - 1], j = 1, 2 \right\}$ is a regular grid for \mathbb{T}^2 defined by positive integers N_1 and N_2 . The 2-D random field under consideration admits a model of a single complex exponential corrupted by additive white complex Gaussian noise, see Sec. 5 in Zhu and Liu (2022). The ratio between the amplitude of the complex exponential and the standard deviation of the noise is $1/\sqrt{2}$. The sample size of the random field is $N_1 \times N_2$, the same as the size of the grid \mathbb{T}_N^2 . Standard biased covariance estimates $\{\hat{\sigma}_k\}_{k \in \Lambda}$ (Stoica and Moses, 2005) are computed from the samples and they play the role of $\Sigma = \{\sigma_k\}_{k \in \Lambda}$ in the dual problem. In addition, the prior $\Psi \equiv \sigma_0$ is a constant.

In the numerical example to be presented next, we take $N_1 = N_2 = 30$, and $n_1 = n_2 = 1$ which defines the index set Λ in (3). Newton's method involves the full Hessian of size 9×9 , and the Newton direction at each iteration is obtained by solving a linear system of equations of the form (30) using Algorithm 2. In contrast, the quasi-Newton method in Zhu and Liu (2022) employs a reduced Hessian of size 5×5 . The convergence of the two methods with respect to the number of iterations are depicted in Fig. 2. It is clear that the true Newton's method converges much more rapidly than the alternative. Although each iteration of the full-Hessian computation takes approximately twice of the time for the quarter Hessian, overall the computational times using the full Hessian and the quarter Hessian are approximately 0.04 and 0.38 seconds, respectively, when the accuracy of the iterate as measured by the distance to the optimal point is within 10^{-8} . Thus, in this example Newton's method is faster then the quasi-Newton method using the quarter Hessian by roughly an order of magnitude.

7. CONCLUSIONS

We have devised a fast Newton solver for the solution of a 2-D spectral estimation problem. The Toeplitz-block Toeplitz structure of the full Hessian of the dual function

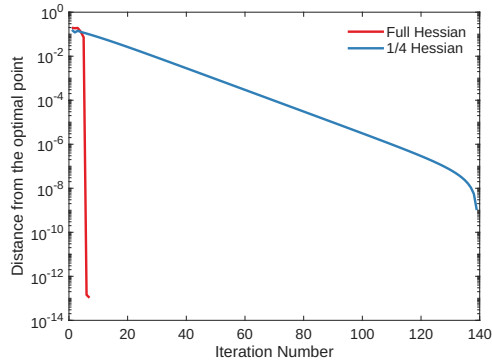


Fig. 2. Full Hessian vs. the quarter Hessian in Newton's method for the solution of the dual problem (6): Euclidean distance between the k -th iterate \mathbf{q}^k and the optimal point \mathbf{q}^* .

is exploited so that an efficient inversion algorithm from the literature can be used upon suitable adaptation. The convergence of the true Newton's method is remarkable in comparison with the quasi-Newton method in a previous work which uses only a quarter Hessian.

REFERENCES

Akaike, H. (1973). Block Toeplitz matrix inversion. *SIAM Journal on Applied Mathematics*, 24(2), 234–241.

Byrnes, C.I., Georgiou, T.T., and Lindquist, A. (2000). A new approach to spectral estimation: A tunable high-resolution spectral estimator. *IEEE Transactions on Signal Processing*, 48(11), 3189–3205.

Byrnes, C.I., Gusev, S.V., and Lindquist, A. (1998). A convex optimization approach to the rational covariance extension problem. *SIAM Journal on Control Optimization*, 37(1), 211–229.

Byrnes, C.I., Gusev, S.V., and Lindquist, A. (2001). From finite covariance windows to modeling filters: A convex optimization approach. *SIAM Review*, 43(4), 645–675.

Engels, F., Heidenreich, P., Zoubir, A.M., Jondral, F.K., and Wintermantel, M. (2017). Advances in automotive radar: A framework on computationally efficient high-resolution frequency estimation. *IEEE Signal Processing Magazine*, 34(2), 36–46.

Ferrante, A., Masiero, C., and Pavon, M. (2012). Time and spectral domain relative entropy: A new approach to multivariate spectral estimation. *IEEE Transactions on Automatic Control*, 57(10), 2561–2575.

Ferrante, A., Pavon, M., and Ramponi, F. (2008). Hellinger versus Kullback–Leibler multivariable spectrum approximation. *IEEE Transactions on Automatic Control*, 53(4), 954–967.

Georgiou, T.T. and Lindquist, A. (2003). Kullback–Leibler approximation of spectral density functions. *IEEE Transactions on Information Theory*, 49(11), 2910–2917.

Hörmander, L. (1990). *An introduction to Complex Analysis in Several Variables*. North Holland, 3rd edition.

Kreutz-Delgado, K. (2009). The complex gradient operator and the \mathbb{CR} -calculus. arXiv preprint: <https://arxiv.org/abs/0906.4835>.

Lindquist, A. and Picci, G. (2015). *Linear Stochastic Systems: A Geometric Approach to Modeling, Estimation and Identification*, volume 1 of *Series in Contemporary Mathematics*. Springer-Verlag Berlin Heidelberg.

Lindquist, A. and Picci, G. (2016). Modeling of stationary periodic time series by ARMA representations. In *Optimization and Its Applications in Control and Data Sciences: In Honor of Boris T. Polyak's 80th Birthday*, 281–314. Springer.

Ringh, A., Karlsson, J., and Lindquist, A. (2015). The multidimensional circulant rational covariance extension problem: Solutions and applications in image compression. In *54th Annual Conference on Decision and Control (CDC)*, 5320–5327. IEEE.

Ringh, A., Karlsson, J., and Lindquist, A. (2018). Multidimensional rational covariance extension with approximate covariance matching. *SIAM Journal on Control and Optimization*, 56(2), 913–944.

Stoica, P. and Moses, R. (2005). *Spectral Analysis of Signals*. Pearson Prentice Hall, Upper Saddle River, NJ.

Wax, M. and Kailath, T. (1983). Efficient inversion of Toeplitz-block Toeplitz matrix. *IEEE Transactions on Acoustics, Speech, and Signal Processing*, 31(5), 1218–1221.

Zhu, B., Ferrante, A., Karlsson, J., and Zorzi, M. (2019). Fusion of sensors data in automotive radar systems: A spectral estimation approach. In *58th IEEE Conference on Decision and Control (CDC 2019)*, 5088–5093. IEEE.

Zhu, B., Ferrante, A., Karlsson, J., and Zorzi, M. (2021a). M^2 -spectral estimation: A flexible approach ensuring rational solutions. *SIAM Journal on Control and Optimization*, 59(4), 2977–2996.

Zhu, B., Ferrante, A., Karlsson, J., and Zorzi, M. (2021b). M^2 -spectral estimation: A relative entropy approach. *Automatica*, 125. doi: 10.1016/j.automatica.2020.109404.

Zhu, B. and Liu, J. (2022). A fast robust numerical continuation solver to a two-dimensional spectral estimation problem. *IET Control Theory & Applications*, 16(9), 902–915.

Zhu, B., Liu, J., Lai, Z., and Qian, T. (2023). Sampling gaussian stationary random fields: A stochastic realization approach. *ISA Transactions*, 142, 386–398.

Zhu, B. and Zorzi, M. (2023). A well-posed multidimensional rational covariance and generalized cepstral extension problem. *SIAM Journal on Control and Optimization*, 61(3), 1532–1556.

Zhu, B. and Zorzi, M. (2024a). Analyzing the impact of regularization on REMSE. *Automatica*, 163. doi: 10.1016/j.automatica.2024.111605.

Zhu, B. and Zorzi, M. (2024b). On the statistical consistency of a generalized cepstral estimator. *IEEE Transactions on Automatic Control*, 69(9), 5775–5787.

Zohar, S. (1969). Toeplitz matrix inversion: The algorithm of W. F. Trench. *Journal of the ACM*, 16(4), 592–601.

Zorzi, M. (2014a). A new family of high-resolution multivariate spectral estimators. *IEEE Transactions on Automatic Control*, 59(4), 892–904.

Zorzi, M. (2014b). Rational approximations of spectral densities based on the alpha divergence. *Mathematics of Control, Signals, and Systems*, 26(2), 259–278.